# Correlations between the Cosmic Microwave Background and Infrared Galaxies

B. Scheiner and J. McCoy
*Department of Physics and Astronomy, University of Iowa, Iowa City, IA 52240*

## ABSTRACT

We report a correlation analysis between *WISE* infrared galaxy density and the 7-year *WMAP* data release for the $K$, $Ka$, $Q$, $V$ and $W$ bands at $8.9\sigma$, $5.5\sigma$, $3.4\sigma$, $1.7\sigma$ and $1.8\sigma$ detection levels respectively. Galaxy densities were constructed from the *WISE* catalog using magnitude and color cut-offs, where the median of the redshift distribution was inferred to be z=0.148 from the work of Goto, Szapudi & Granett (2012). An excess signal in the cross correlation at a multipole moment of $\ell \approx 10$ is consistent with the detection of the late time integrated Sachs-Wolfe effect at the inferred redshift. The cross power spectra are in agreement for *WMAP* $V$ and $W$ bands, while discrepancies in the $K$, $Ka$, and $Q$ bands are likely due to contamination in the *WMAP* data from Galactic emission.

*Subject headings:* cosmic microwave background – the Integrated Sachs-Wolfe effect – dark energy

## 1. Introduction

ΛCDM is considered to be the standard model of Big Bang cosmology, featuring dark energy (DE), represented by the cosmological constant Λ, and cold dark matter. From distant Type Ia supernova observations, it has been shown that the Hubble expansion of the Universe becomes DE-dominated at redshift $z \sim 0.5$ (Perlmutter et al. 1999). At this point, the evolution of the scale factor of the Universe switches from $a(t) \propto t^{2/3}$, while it is matter-dominated, to $a(t) \propto e^{Ht}$, where the Hubble constant is $H = \sqrt{\Lambda/3}$. As a result, the self-gravitation of large-scale structure starts to become over-powered by this recent accelerated expansion, and thus their potential wells gradually decay. Sachs & Wolfe (1967) postulated that if potential wells should decay over time scales shorter than a photon crossing time, then traces of this effect will be observable in the cosmic microwave background (CMB) radiation. The basic physical picture of this scenario, known as the late-time integrated Sachs-Wolfe (ISW) effect, or the Rees-Sciama effect (Rees & Sciama 1968), is outlined in the following.

As a photon enters a gravitational potential well, it is initially blueshifted. If DE can be neglected, the gravitational redshift due to the photon's exit exactly balances the initial energy boost, and there is no net effect. However, if we consider our Universe at sufficiently low redshift, when it is DE-dominated, a photon's exit from a potential well that decays on a short enough time scale will not fully compensate for the initial energy boost. As a result, a photon crossing the well will be left with a net blueshift. Conversely, a photon that crosses a decaying void (i.e., a potential hill) will be left with a net redshift. It follows that these mechanisms of decaying potential should be uniquely caused by the presence of DE if the Universe is flat (Crittenden & Turok 1996).

When studying the effects of CMB photons crossing decaying gravitational potential wells (hills), the additional blueshift (redshift) corresponds to a small relative increase (decrease) in CMB temperature. The CMB has primary temperature anisotropies on small angular scales due to physical processes at the time of recombination ($z \sim 1100$). These anisotropies are predominately on the scale of 1° or less due to the horizon size at recombination and the speed of sound in the primordial photon-baryon fluid. However, the ISW

effect serves as a secondary source of temperature anisotropy for CMB photons at larger angular sizes (typically $\sim 5^\circ$), corresponding to the scale of structure at DE-dominated redshifts. Other mechanisms for secondary anisotropies of CMB exist, including effects due to gravitational lensing and the Sunyaev-Zel'dovich (SZ) effect, which distorts anisotropies on small angular scales through inverse Compton scattering.

Here we study CMB anisotropies from the most recent *Wilkinson Microwave Anisotropy Probe (WMAP)* data release (Komatsu et al. 2011). Because of their relatively weak amplitudes, low-multipole anisotropies due to the ISW effect are difficult to isolate. However, the ISW signal can be detected statistically by performing a cross-correlation between anisotropies in the CMB and in the mass distribution at some DE-dominated redshift. A detailed description and theoretical model of this method are presented in Crittenden & Turok (1996). The larger $\Lambda$ is, the earlier the Universe will become DE-dominated, and the more pronounced the ISW effect will be at a given redshift. Therefore performing this cross-correlation is a way to directly detect the presence of DE and constrain the value of $\Lambda$. Mass anisotropies at low redshift can be inferred from studying the number density of galaxies across the sky. Among the first to attempt this cross-correlation was Ganga et al. (1993) who used data from the Cosmic Background Explorer (COBE) and a 170 GHz partial-sky survey. Additionally, Bennett et al. (1993) carried out an analysis with COBE data and X-ray maps from the High Energy Astronomy Observatory 1 (HEAO-1) satellite. However, these studies did not provide a clear ISW signal.

Cross-correlation between *WMAP* data and observed matter anisotropies has been done previously for many sky surveys, including Sloan Digital Sky Survey (SDSS) luminous red galaxies (Scranton et al. 2003; Padmanabhan et al. 2005; Granett, Neyrinck & Szapudi 2009), SDSS quasars (Giannantonio et al. 2006), infrared galaxies from the Two Micron All-Sky Survey (2MASS) (Afshordi, Loh & Strauss 2004; Rassat et al. 2007; Francis & Peacock 2010), radio galaxies from the NRAO VLA Sky Survey (NVSS) (Bough & Crittenden 2004; Nolta et al. 2004; Raccanelli et al. 2008), the X-ray background from the HEAO-1 satellite (Bough & Crittenden 2004), optical galaxies from the Automatic Plate Measuring Machine Survey (APM) (Fosalba & Gaztaña 2010) and more. Others have combined many sky surveys in their analysis including Giannantonio et al. (2008) and Ho et al. (2008), providing a $\sim 4\sigma$ detection level. A benefit of performing this study for many different sky surveys is that each typically corresponds to a distribution of galaxies at a different median redshift. Probing the ISW signal at many different redshifts helps to piece together a picture of how DE causes structure to decay over time.

In this paper we use *Wide-field Infrared Survey Explorer Survey (WISE)* detected galaxies (Wright et al. 2010) to perform a cross-correlation between anisotropies in the CMB and the mass distribution in the form of galaxy counts. We closely follow the recent work of Goto, Szapudi & Granett (2012) in an effort to reproduce their results and to detect the ISW signal using a larger part of the sky. Later we will explain that we are probing the ISW effect at a median redshift of $z = 0.15$. Section 2 of this paper addresses our general mathematical procedures for calculating the correlation, while Section 3 concerns the details on the *WMAP* and *WISE* observations used. In Section 4 we present our results and describe our data analysis. We discuss our results and conclusions in Section 5.

## 2. Mathematical Background & Methods

When working with all-sky observations, it is convenient to deal with CMB anisotropies by decomposing the relative temperature fluctuations in terms of spherical harmonics $Y_{\ell m}$:

$$\frac{T(\theta,\phi)-\bar{T}}{\bar{T}} = \sum_{\ell=2}^{\infty}\sum_{m=-\ell}^{\ell} a^T_{\ell m} Y_{\ell m}(\theta,\phi) \qquad (1)$$

where $\bar{T} \approx 2.73$ K is the average CMB temperature and $a^T_{\ell m}$ are a set of coefficients calculated from *WMAP* maps to describe the weighting of each multipole moment. It is standard that the monopole and dipole terms are removed, so we start the summation with $\ell = 2$. This removes unwanted signal due to motion realtive to the CMB

rest frame. The angular power spectrum,

$$(2\ell+1)C_\ell^{TT} = \sum_{m=-\ell}^{\ell} a_{\ell m}^T a_{\ell m}^{T*} \quad (2)$$

of the CMB is known to peak at $\ell \approx 200$, corresponding to the $\sim 1^\circ$ scale of anisotropy due to acoustic sound peaks discussed previously. Crittenden & Turok (1996) have demonstrated that the ISW effect should contribute to multlipoles $\ell < 100$, but most dramatically for $\ell \approx 10$. For this reason we will not consider multipole moments for $\ell > 200$.

In an analogous fashion, galaxy number per pixel $N_g(\theta, \phi)$, measured from *WISE* data, is also decomposed in terms of spherical harmonics:

$$N_g(\theta,\phi) = \sum_{\ell,m} a_{\ell m}^g Y_{\ell m}(\theta,\phi) \quad (3)$$

where $a_{\ell m}^g$ are a set of weighting coefficients for galaxy counts at each multipole. The upper limit of $\ell$ is set by the counting bin size. Likewise, the galaxy-galaxy power spectrum is

$$(2\ell+1)C_\ell^{gg} = \sum_{m=-\ell}^{\ell} a_{\ell m}^g a_{\ell m}^{g*} \quad (4)$$

where we expect correlation at low multipoles as the Universe approaches homogeneity on very large scales. Once both sets of coefficients, $a_{\ell m}^T$ and $a_{\ell m}^g$, are found from the analysis of the *WMAP* and *WISE* data respectively, it is straightforward to compute the cross-correlation between CMB anisotropies and galaxy number density:

$$(2\ell+1)C_\ell^{Tg} = \sum_{m=-\ell}^{\ell} a_{\ell m}^T a_{\ell m}^{g*}. \quad (5)$$

Ultimately we want to cross-correlate CMB fluctuations with the distribution of matter at a given redshift. This is represented by relative mass density contrast, $\delta_m = (\rho - \bar{\rho})/\bar{\rho}$, where $\bar{\rho}$ is the mean cosmic matter density in the Universe. This is related to gravitational potential $\Phi$ through Poisson's equation

$$\nabla^2\Phi = 4\pi G\rho = 4\pi G a^2 \bar{\rho}\delta_m \quad (6)$$

where $a$ is the scale factor of the Universe. From studying the *WISE* survey however, we can only directly obtain information about relative galaxy number density contrast, defined as $\delta_g = (N_g - \bar{N}_g)/\bar{N}_g$, where $\bar{N}_g$ is the mean number of galaxies per pixel. To take into account the actual distribution of matter due to the presence of dark matter, we must correct $\delta_g$ for galaxy bias, $b_g$, to obtain $\delta_m$.

The observed value of $\delta_g$ is related to $\delta_m$ by

$$\delta_g(\theta,\phi) = \int b_g(z)\frac{dN(z)}{dz}\delta_m(\theta,\phi,z)\mathrm{d}z \quad (7)$$

where $dN/dz$ is the galaxy number distribution over redshift (Giannantonio et al. 2008). This was determined from a cross-match of the *WISE* with the Galaxy And Mass Assembly (GAMA)[1] survey, a spectroscopic redshift survey (Driver et al. 2011), by Goto, Szapudi & Granett (2012). From this, the median redshift of the *WISE* survey was found to be $z = 0.148$, which can be safely be considered to be DE-dominated. The amplitude of the galaxy-galaxy power spectrum scales with $b_g^2$, and in Section 4 we fit a theory curve from Goto, Szapudi & Granett (2012) to our *WISE* galaxy auto-correlation data to estimate a value for galaxy bias.

## 3. Observations

Because we are dealing with all-sky surveys, projection effects must be eliminated. To do this we work with data in HEALPIX[2] format. This allows us to work with the celestial sphere divided into pixels of equal area tessellations. In terms of the HEALPIX resolution parameter, $N_{side}$, the celestial sphere is partitioned into $12N_{side}^2$ pixels placed on $4N_{side}-1$ rings of constant latitude. For both sets of data we use parameter $N_{side} = 512$, corresponding exactly to the upper multipole $\ell$ limit considered for binning. In the following we explain the details concerning the *WMAP* and *WISE* observations.

### 3.1. *WMAP*

We obtained the *WMAP* 7-year data set consisting of five standard CMB bands, $K$, $Ka$, $Q$, $V$ and $W$, corresponding to 22, 30, 40, 60 and

[1] http://www.gama-survey.org/

[2] Hierarchical Equal Area isoLatitude Pixelization, see http://healpix.jpl.nasa.gov

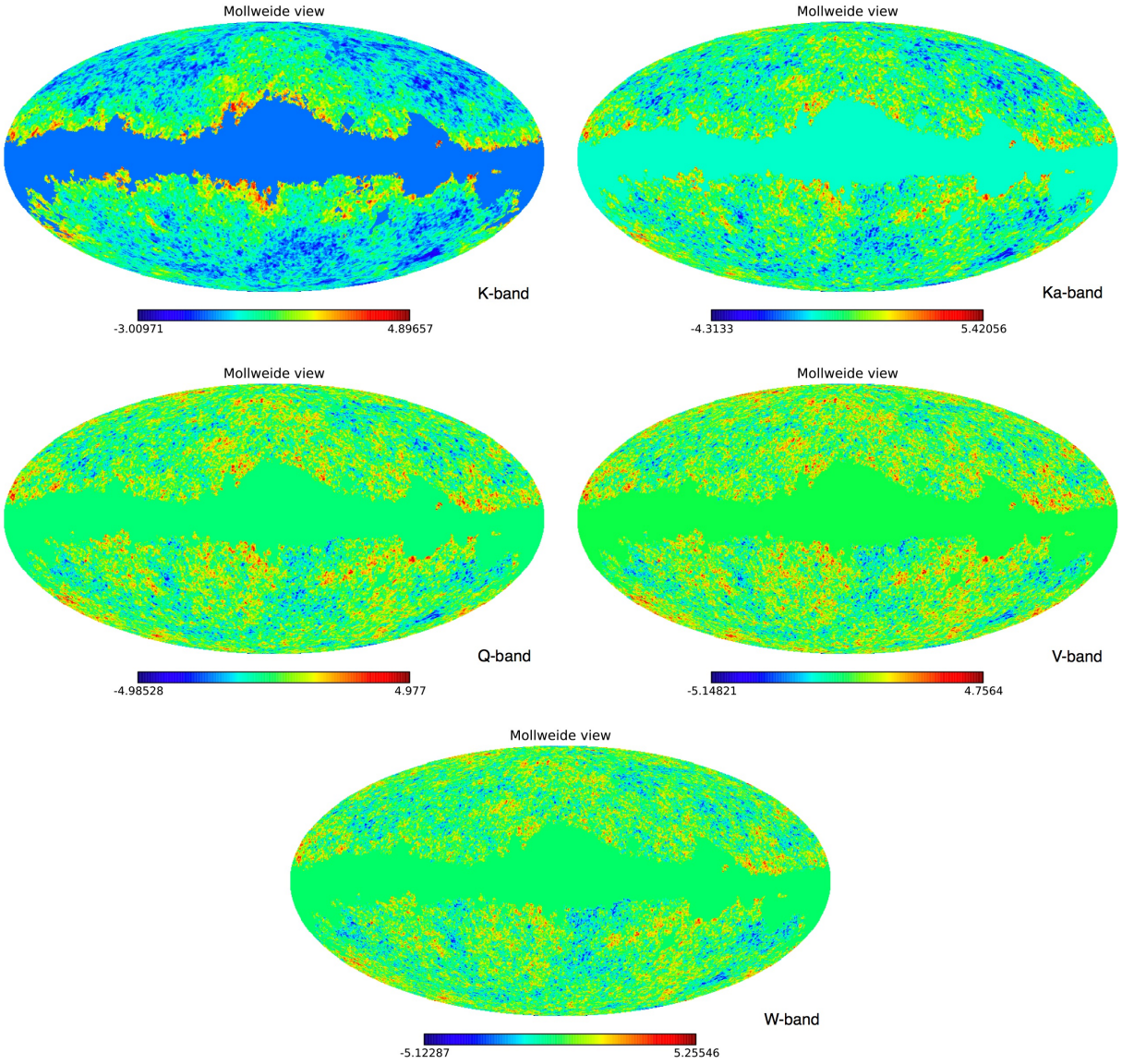


Fig. 1.— Relative temperature fluctuations in the CMB seen with the *WMAP* survey in five bands, in order of increasing frequency. Although the *WMAP* mask is applied to each, foreground contamination is still seen, predominately in the $K$ and $Ka$ bands.

90 $GHz$ repsectively, with the monopole and dipole terms pre-subtracted (Komatsu et al. 2011). To block unwanted foreground sources from our galaxy, we applied the *WMAP* mask[3] provided by NASA. These five all-sky plots are displayed in Fig. 1, where the *WMAP* mask is seen to be more effective for blocking foreground emission in the $V$ and $W$ bands.

### 3.2. *WISE*

The *WISE* data release consists of observations at wavelengths of 3.4, 4.6, 12 and 22 $\mu$m, dubbed $W1$, $W2$, $W3$ and $W4$ respectively (Wright et al. 2010). To select a uniform distribution of galaxies across the sky, this survey was narrowed down with magnitude and color cut-offs. Because the *WISE* data is deeper near the celestial poles, we chose a magnitude cut-off of $W1 < 15.2$. In an effort to remove foreground stars we constrained our search to colors of $W1 - W2 > 0.2$. Requiring $W2 - W3 > 2.9$ further removes foreground stars, but it comes at the price of removing some galaxies (Wright et al. 2010). These same search parameters were used by Goto, Szapudi & Granett (2012). After these color cut-offs were implemented however, large foreground structure was still seen in the *WISE* all-sky map. To resolve this, we manually removed these sources using with the NASA ADS's Dexter[4], a data extraction applet. This allowed us to extract a list of coordinates of the unwanted sources, masking the surrounding eight pixels of each.

Furthermore, we cut out the zone of avoidance ($|b| > 10^\circ$) and additionally applied the *WMAP* mask to cut out the bulk of the stars in our galaxy. We then binned galaxy counts into pixels according to $N_{side} = 512$ and smoothed this galaxy number density with a Gaussian with a FWHM of $0.5^\circ$. This is justified because the ISW is only expected to affect angular sizes of $\sim 5^\circ$ corresponding to multipoles $\ell < 100$. The all-sky map of binned *WISE* galaxies after all source selection is seen in Fig. 2.

[3]http://map.gsfc.nasa.gov/news/

[4]http://www.adass.org/adass/proceedings/adass00/P2-45/

## 4. Results

As an intermediate check point before presenting the CMB-galaxy cross-correlation, we plot the power spectrum of each individually. Because we are interested in detecting the ISW signal, not affecting multipoles $\ell > 100$, both were computed up through only $\ell = 512$. The W-band CMB power spectrum $C_\ell^{TT}$ as described in Eq. 2, is seen in Fig. 3. As expected, there is a peak at $\ell \approx 200$, as a result of the sound speed at recombination. Fig. 4 shows the power spectrum of *WISE* galaxy counts $C_\ell^{gg}$ (Eq. 4) overlaid with a curve representing a theoretical galaxy density power spectrum computed based currently accepted $\Lambda$CDM model parameters by Goto, Szapudi & Granett (2012). The plot of $C_\ell^{gg}$ shows that structure is correlated at low multipoles as the Universe approaches homogeneity, but becomes uncorrelated as $\ell$ increases. Coordinates of the theory curve were extracted using the applet Dexter, where a bias factor of $b_g = 1.06 \pm 0.005$ has already been applied by Goto, Szapudi & Granett (2012). In an effort to fit this curve to our results for $C_\ell^{gg}$, we scaled it by a factor of 1.7 corresponding to to a bias factor estimate of $b_g \approx 1.06 \times \sqrt{1.7} \approx 1.4$.

We made use of an existing algorithm in HEALPIX to perform the cross-correlation described in Eq. 5. However, here the $a_{\ell m}$ coefficinets from CMB anisotropies and galaxy counts are normalized according to

$$\frac{T(\theta,\phi) - \bar{T}}{\sigma_T} = \sum_{\ell,m} a_{\ell m}^T Y_{\ell m}(\theta,\phi) \qquad (8)$$

and

$$\frac{N_g(\theta,\phi) - \bar{N_g}}{\sigma_g} = \sum_{\ell,m} a_{\ell m}^g Y_{\ell m}(\theta,\phi) \qquad (9)$$

where $\sigma_T$ and $\sigma_g$ are the standard deviations of CMB temperature anisotropies and galaxy number density, respectively. In an effort to better see the ISW signal at low multipoles, we chose to bin at roughly logarithmic intervals. Because the angular size of the *WMAP* mask and the blocked out zone of avoidance corresponds to $\ell \sim 180^\circ/\theta \sim 6$ (Goto, Szapudi & Granett 2012), we excluded multipoles lower than this in our calculation. As previously stated, the ISW effect is not expected to occur for multipoles above $\ell \approx 100$, so we

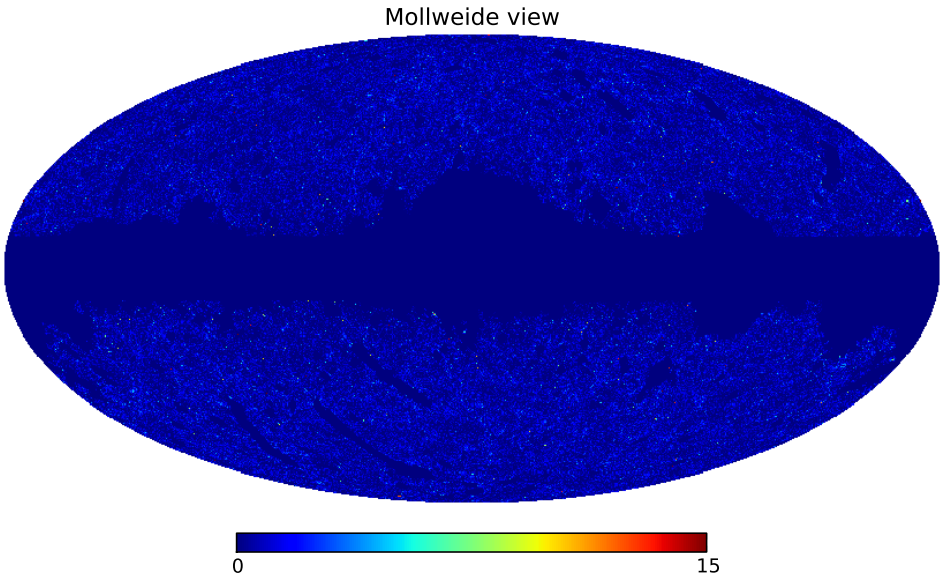


Fig. 2.— Binned number density of *WISE* galaxies over the sky after initial foreground source removal and the exclusion of the zone of avoidance. Color scale shows the number of detected galaxies per pixel. The *WMAP* mask to remove foreground sources has been applied.

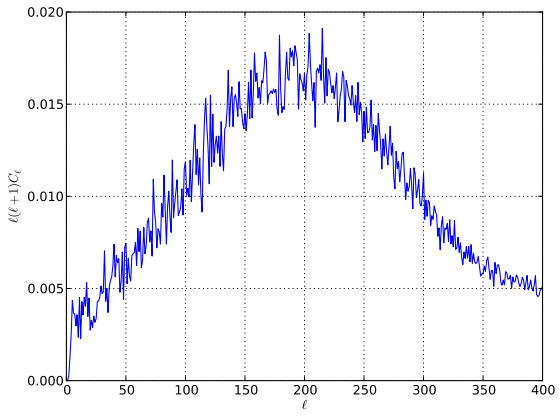


Fig. 3.— Power spectrum of *WMAP* survey in the W-band. The *WMAP* mask has been applied and the monopole and dipole terms were pre-subtracted. A peak at $\ell \approx 200$ is seen, as a result of acoustic peaks at the time of recombination.

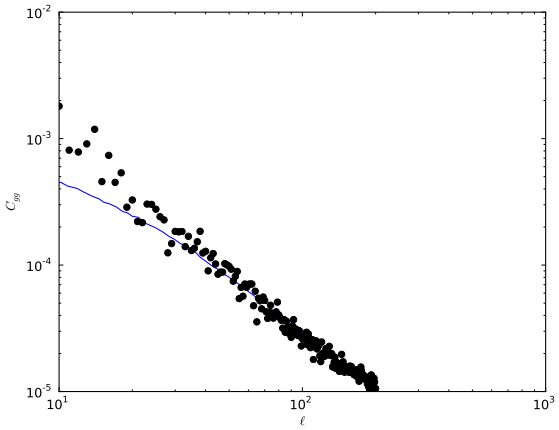


Fig. 4.— *WISE* galaxy-galaxy power spectrum, overlaid with a theoretical galaxy density power spectrum. The theory curve must be matched with $C_\ell^{gg}$, to correct for galaxy bias.

used bin boundaries: $\ell$ = 5, 7, 10, 15, 21, & 30. The cross-correlation between each *WMAP* band and *WISE* galaxy counts is presented in Fig. 5. These plots are also overlaid with curves representing theory according to Goto, Szapudi & Granett (2012), which were obtained digitally with Dexter. Methods for error analysis are described in the following.

Because spatial phase information is not preserved when computing auto-correlations, many CMB maps can produce identical power spectra. The phase information contained in $a_{\ell m}$ coefficients however, do contribute to cross-correlations. We used SYNFAST[5], a program within HEALPIX, to produce 1,000 random statistically equivalent CMB maps, each with different phase information. We then computed the cross-correlation of each with the *WISE* data and calculated the standard deviation for each multipole. This was done for each *WMAP* band serving as the error bars seen in Fig. 5. From this, we find detection levels of $8.9\sigma$, $5.5\sigma$, $3.4\sigma$, $1.7\sigma$ and $1.8\sigma$ for cross-correlation in the $K$, $Ka$, $Q$, $V$ and $W$ bands respectively, for the multipole range $7 < \ell < 15$.

## 5. Conclusion

We have measured the cross-correlation between *WISE* infared galaxies and the CMB from the *WMAP* $K$, $Ka$, $Q$, $V$, & $W$ bands. An excess signal at $\ell \approx 10$ in all five *WMAP* bands is in agreement with what is expected due to the ISW effect at a redshift of z=0.148. This result is consistent with the detection of the ISW effect in *WISE* data by Goto, Szapudi & Granett (2012) while including a larger portion of the sky. Although the detected signal is consistent with the ISW effect, a false signal is likely the result of contamination in the *WISE* or *WMAP* data.

Contamination of galaxy counts in the *WISE* map due to nearby Galactic emission or other local structure on the sky can cause excess power at large spatial scales, correspoding to low multipoles. We are confident this is not the case for the *WISE* galaxy density map. Nearby structure as well as bright point sources were masked out before the correlation with *WMAP* data. The *WISE* galaxy density maps are visually absent of any large scale gradient.

One cause for concern is the differing levels of the signal in the cross-correlation between *WMAP* bands. This can be explained by the apparent contamination of the $K$ and $Ka$ bands, and to a lesser extent, the $Q$ band. This contamination can be seen near the zone of avoidance and is due to the incomplete masking of emission in those bands. The power level in the cross correlation seems to increase with the amount of visible contamination, while the $V$ and $W$ band correlations, with no contamination, are in agreement.

The detection of the Integrated Sachs-Wolfe effect with *WISE* selected galaxies confirms that the Universe must have been DE-dominated at $z = 0.148$. This is well within agreement with the Universe switching from being matter-dominated, to being DE-dominated at $z \sim 0.5$ according to the observations of Perlmutter et al. (1999) and of currently accepted $\Lambda$CDM theory. This study provides another piece of evidence for the accelerated expansion of the Universe, and along with cross-correlation studies between CMB anisotropies and other sky all-surveys, will help to further constrain $\Lambda$ and the effect it has on the gravitational potential of large-scale structure.

[5]http://healpix.jpl.nasa.gov/html/facilitiesnode14.htm

## REFERENCES


Afshordi, N., Loh, Y., & Strauss, M. A., 2004, Phys. Rev. D, 69, 083524

Bennett, C., et al. 1993, ApJ, 414, L77

Cooray, A., 2002, Phys. Rev. D, 65, 103510

Bough, S., & Crittenden, R., 2004, Nature, 427, 45

Crittenden, R. G., & Turok, N., 1996, Phys. Rev. Lett., 76, 575

Driver, S. P., et al. 2011, MNRAS, 413, 971

Fosalba, P., & Gaztañaga, E., 2004, MNRAS, 350, L37

Francis, C. L., & Peacock J. A., 2010, MNRAS, 402, 2

Ganga, K., et al., 1993, ApJ, 410, L57

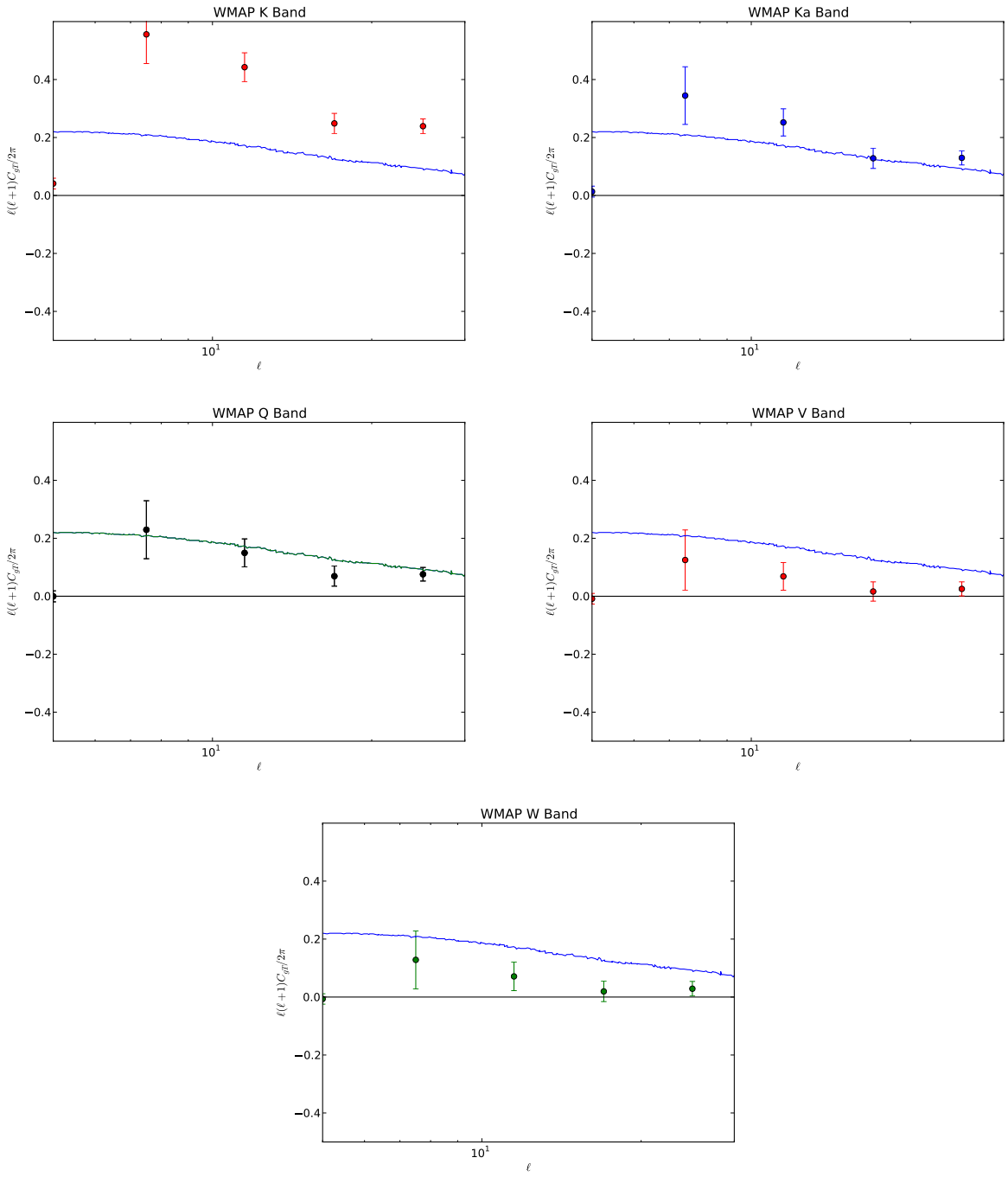


Fig. 5.— Cross-correlation in the five *WMAP* bands, with boundaries at $\ell$ = 5, 7, 10, 15, 21, & 30 with theory curves overlaid.

Giannantonio, T., Crittenden, R., Nichol, R., & Ross, A. J. 2012, MNRAS, 426, 2581

Giannantonio, T., et al. 2008, Phys. Rev. D, 77, 12, 123520

Giannantonio, T., et al. 2006, Phys. Rev. D, 74, 12, 063520

Goto, T., Szapudi, I., & Granett R. G., 2012, MNRAS, 422, L77

Granett, B. R., Neyrinck, M. C., & Szapudi, I., 2009, ApJ, 701, 414

Ho, S., et al. 2008, Phys. Rev. D, 78, 043519

Komatsu, E., et al. 2011, ApJS, 192, 18

Nolta, M. R., et al. 2004, ApJ, 608, 610

Padmanabhan, N., et al. 2005, Phys. Rev. D, 72, 043525

Perlmutter, S., et al. 1999, ApJ, 517, 565

Raccanelli, A., et al. 2008, MNRAS, 386, 2161

Rassat, A., et al. 2007, MNRAS, 377, 1085

Rees, M. J., & Sciama, D. W., 1968, Nature, 217, 511

Sachs, R. K., & Wolfe, A. M., 1967, ApJ, 147, 73S

Scranton, R., et al. 2003, arXiv:astro-ph/0307335

Wright, E. L., et al. 2010 AJ, 140, 6, 1868

This 2-column preprint was prepared with the AAS LaTeX macros v5.2.